

A numerical approach for solving the nonlinear Van der Pol system of heartbeat model

Muhammad Umar¹, Zulqurnain Sabir^{2,*}, Fazli Amin³, Juan L.G. Guirao⁴, Muhammad Asif Zahoor Raja⁵

^{1,*}Department of Mathematics and Statistics, Hazara University, Mansehra, Pakistan

Emails: umar_maths@hu.edu.pk, humar922015@gmail.com

²Department of Mathematics and Statistics, Hazara University, Mansehra, Pakistan

Emails: zulqurnain_maths@hu.edu.pk, zulqurnainsabir@gmail.com, +923335868270

³Department of Mathematics and Statistics, Hazara University, Mansehra, Pakistan

Email: fazliamin@hu.edu.pk

²Department of Applied Mathematics and Statistics, Technical University of Cartagena, Hospital de Marina 30203-Cartagena, Spain

Email: juan.garcia@upct.es

⁵Department of Electrical and Computer Engineering, COMSATS University Islamabad, Attock Campus, Attock 43600, Pakistan

Email: muhammad.asif@ciit-attock.edu.pk

Abstract: In the present work, a numerical technique is established for numerical treatment of nonlinear Van der Pol system of heartbeat model (VPS-HBM) using feedforward artificial neural networks (ANNs) optimized with particle swarm optimization (PSO) hybridize through active-set algorithm (ASA). The system mathematical modeling is assembled using ANN by defining an unknown weights and unsupervised error; PSO in the network is used as global parameter while ASA is used for local enhancement. Design technique is used for the numerical treatment of the dynamics of VPS-HBM by fluctuating the pulse shape adjustment factor, external forcing factor and damping coefficients while the fixed value of ventricular contraction period is taken. To establish the correctness of the present scheme, Adams numerical method is applied for comparison of the proposed solutions. The statistical analysis based on of mean absolute deviation, variance account for, Theil's inequality coefficient demonstrate its applicability, reliability and effectiveness.

Keywords: Particle swarm optimization, heartbeat model, artificial neural networks, active-set, statistical analysis.

1. Introduction

The recent study is about the nonlinear Van der Pol system of heartbeat model (VPS-HBM)) using the strength of artificial neural networks (ANNs) optimized with the combination of particle swarm optimization (PSO) and active set algorithm (ASA). To represent the heart functions [1-2] theoretically, the Van der Pol (VP) oscillatory systems have been introduced like as relaxation, chaotic behavior, periodicity and bifurcations [3]. The mathematical illustration of VP model of heart dynamics in the form of nonlinear oscillator is a second order nonlinear equation and written as [4]:

$\ddot{u} + a(u - v_1)(u - v_2)\dot{u} + \frac{u(u+d)(u+e)}{de} = g(t),$	(1)
$u(0) = C_1, \quad \dot{u}(0) = C_2.$	

Where length of heart fiber is represented by u , the factor a is used to modify the heartbeat pulse shape, ventricular contraction period is represented by e . The parameters v_1 and v_2 used for composing an asymmetric span that modify the damping term, factor d is used to replace a cubic term by the harmonic forcing in standard VP equation and $g(t)$ is the external forcing factor.

Many analytical and numerical solvers have been presented for finding the approximate solution of model (1). In this regard, few potential techniques are Adomian decomposition technique [5], homotopy analysis technique [6], He's parameter-expanding technique [7], linearization technique [8] and Laplace decomposition technique [9] etc. These all-existing processes have their particular applicability, intrinsic worth, limitations and drawbacks, however, besides the deep-rooted strength of the stochastic numerical solvers, these techniques are rarely used to solve momentous bioinformatics systems based on VP heart dynamics system (1).

Stochastic numerical solvers based on ANNs are reflected to be efficient, precise and consistent measures for solving efficiently optimization models arising in numerous fields [10–14]. Some recent ANNs based artificial intelligence method contain inverse kinematics problems [15], cell biology [16], nonlinear Troesch's problem [17], nonlinear prey-predator models [18], power [19], uncertainties in computational mechanics [20], thinfilm flow [21], nonlinear singular Thomas-Fermi systems [22], fuzzy differential equations [23], heat conduction model of human head [24], nonlinear doubly singular systems [25], transistor-level uncertainty quantification [26], nanofluidics problems [27], nonlinear second order multi-point boundary value problems [28], control systems [29] and energy [30]. The above work motivated the author to exploit and explore the stochastic solvers strength for designing an accurate, alternate, reliable, robust computing procedure for the dynamical VPS-HBM.

In the present work, stochastic solver based on ANNs optimized with the combinations of PSO-ASA is designed to examine the VP dynamics of heartbeat model (1) using the hybrid of PSO-ASA. To check the accuracy of the present scheme, Adams method (AM) is used as a reference solution. Three scenarios of VP model (1) has been taken by keeping fix ventricular contraction period value and varying the values of damping coefficients and pulse shape modification factor.

2. Heart modeling

A brief explanation related to VP systems signified in Eq. (1) is given in this section. The VP system was introduced initially for relaxation oscillator description in the modeling of electronic circuits [31] and has been frequently used in theoretical cardiac rhythm models. The mathematical form of VP heart classical model based on nonlinear oscillator [32] is written as:

$\ddot{u} + a(u^2 - 1)\dot{u} + bu = 0,$	(2)
--	------------

where a and b are coefficient constants, associated to duffing and damping system parameters. The differential equation based on VP is used normally in the heart oscillation models. Grudzinski and Zebrowski [33] presented the above VP classical heart model (2). The traditional VP heart model

(1) changed later, and its properties are modified by way of the summation over joining fixed points, stable and saddle node at $u = -2d$ and $u = -d$, respectively. The VPS-HBM with restructured unsymmetrical damping terms associated in imitation of the voltage is devoted as:

$\ddot{u} + a(u^2 - \lambda)\dot{u} + \frac{u(u+2d)(u+d)}{d^2} = 0.$	(3)
--	-----

The association into these couple fixed points does not change; therefore, model (3) is amended by the commencement regarding a current parameter e that is responsible for the modification of depolarization period as:

$\ddot{u} + a(u^2 - \lambda)\dot{u} + \frac{u(u+d)(u+e)}{de} = 0.$	(4)
--	-----

Equation (4) was similarly updated by changing the damping time period $a(u^2 - \lambda)$ with $(u - v_1)(u - v_2)$, written as:

$\ddot{u} + a(u - v_1)(u - v_2)\dot{u} + \frac{u(u+d)(u+e)}{de} = 0.$	(5)
---	-----

The condition $v_1 v_2 < 0$ ought to satisfy in accordance with hold the self-oscillatory features concerning the system. Furthermore, the updated model (5) has the capacity to simulate the fundamental physiological properties regarding a normal heart pacemaker. The forcing factor or external pacemaker $g(t)$, system (5) becomes as:

$\ddot{u} + a(u - v_1)(u - v_2)\dot{u} + \frac{u(u+d)(u+e)}{de} = g(t).$	(6)
--	-----

The Eq. (6) is the nonlinear VP oscillator-based heart model in accordance with instruction the characteristic of cardiac rhythm.

3.1. Present methodology

Neural network mathematical model (1) is framed by exploiting the approximation theory strength in the form of continuous mapping. These solution networks $u(t)$ and its derivatives are given below. The graphical abstract and pseudocode of the present scheme are provided in Fig. 1 and Table 1 respectively.

$\hat{u}(t) = \sum_{j=1}^m \alpha_j p(\xi_j t + \beta_j),$	(7)
$\hat{u}'(t) = \sum_{j=1}^m \alpha_j \dot{p}(\xi_j t + \beta_j),$	

$\hat{u}(t) = \sum_{j=1}^m \alpha_j \ddot{p}(\xi_j t + \beta_j),$	
\vdots	
$\hat{u}^{(n)}(t) = \sum_{j=1}^m \alpha_j p^{(n)}(\xi_j t + \beta_j).$	

Where the values are $\alpha = [\alpha_1, \alpha_2, \alpha_3, \dots, \alpha_m]$, $\xi = [\xi_1, \xi_2, \xi_3, \dots, \xi_m]$ and $\beta = [\beta_1, \beta_2, \beta_3, \dots, \beta_m]$. Using log-sigmoid function $p(t) = 1/(1 + \exp(-t))$, which is an activation function, set of networks (7) with its derivatives are updated as:

$\hat{u}(t) = \sum_{j=1}^m \alpha_j \left(\frac{1}{1 + \exp(-\xi_j t - \beta_j)} \right),$	
$\hat{u}' = \sum_{j=1}^m \alpha_j \xi_j \left(\frac{\exp(-\xi_j t - \beta_j)}{(1 + \exp(-\xi_j t - \beta_j))^2} \right),$	(8)
$\hat{u}'' = \sum_{j=1}^m \alpha_j \xi_j^2 \left(\frac{2 \exp(-2\xi_j t - 2\beta_j)}{(1 + \exp(-\xi_j t - \beta_j))^3} - \frac{\exp(-\xi_j t - \beta_j)}{(1 + \exp(-\xi_j t - \beta_j))^2} \right),$	
\vdots	

To construct the model (1), the set of network (8) is used. To solve heart dynamics model (1), a fitness/error function in the mean square sense given as:

$E = E_1 + E_2.$	(9)
------------------	------------

Where E_1 and E_2 represent error functions. E_1 is related to VP nonlinear differential equation, while E_2 is used for initial conditions, written as:

$E_1 = \frac{1}{N} \sum_{m=1}^N \left(\hat{u} + a(\hat{u}_m - v_1)(\hat{u}_m - v_2)\hat{u}_m + \frac{\hat{u}_m(\hat{u}_m + d)(\hat{u}_m + e)}{de} - g_m \right),$	(10)
$E_2 = \frac{1}{2}(\hat{u}_m - C_1)^2 + \frac{1}{2}(\hat{u}_m' - C_2)^2.$	(11)

Where $N = \frac{1}{h}$, $\hat{u}_m = \hat{u}(t_m)$, $t_m = mh$ and $g_m = g(t_m)$. Solution for model (1) can be achieved by using trained weights $\mathbf{W} = [\boldsymbol{\alpha}, \boldsymbol{\xi}, \boldsymbol{\beta}]$.

3.2. Optimization process: PSO-ASA

Evolutionary computing a process based on PSO hybrid with ASA, i.e., PSO-ASA, is used in the training of unknown modifiable parameter of ANNs for solving the dynamics of VPS-HBM. PSO are considered an accurate, efficient, robust and reliable techniques evolutionary computing field and widely applied in applied sciences. PSO introduced by Eberhart and Kennedy at the last decade of nineteenth century. PSO is replacement to genetic algorithms [34] and used mainly for optimization due to its short memory requirements [35] and ease of implementation. Some recent possible applications of PSO are multicast routing problem in communication networks [36], solar photovoltaic system [37], clustering high-dimensional data [38], multilevel thresholding [39], energy resource scheduling considering vehicle-to-grid [40], gene selection in cancer classification [41], humanoid robots [42] and collective robotic search applications [43].

Each single candidate result in an optimization model represents a particle. In PSO, the problem is explored by generated particles to form a swarm. For optimal performance of the technique, initial swarms spread in the larger domains. In the swarm, an objective function is defined by using the fitness values of the problem and the iterative process is used to get the optimal solutions. The optimal solutions iteratively obtained by initializing the parameters runs in the PSO algorithm. In the swarm, the position and the velocity is simplified by using its previous local and global best positions are $\mathbf{P}_{L-Best}^{q-1}$ and $\mathbf{P}_{G-Best}^{q-1}$. The updating form of PSO for position and velocity is given as:

$\mathbf{X}_i^q = \mathbf{X}_i^{q-1} + \mathbf{V}_i^{q-1},$	(12)
$\mathbf{V}_i^q = \omega \mathbf{V}_i^{q-1} + l_1 \mathbf{q}_1 (\mathbf{P}_{L-Best}^{q-1} - \mathbf{X}_i^{q-1}) + l_2 \mathbf{q}_2 (\mathbf{P}_{G-Best}^{q-1} - \mathbf{X}_i^{q-1}).$	(13)

Where \mathbf{V}_i and \mathbf{X}_i vectors represent the i^{th} velocity vector and swarm particle, respectively, $\omega \in [0,1]$ shows the inertia weight, l_1 and l_2 are acceleration constants and q_1 and q_2 are random vectors. The velocity vector lie in $[-v_{\max}, v_{\max}]$, where v_{\max} shows the maximum velocity. The performance of the algorithm is stopped due to predefined number of flights.

Active set is a local search algorithm and used in optimization process. ASA is applied in constrained/unconstrained optimization problems. Some recent applications are distributed model predictive control [44], real-time optimal control [45], for solving large-scale non-smooth optimization models with box constraints [46], for online deconvolution of calcium imaging data [47] and for solving large non-negative least squares problems [48]. In the present study, combination of PSO-ASA is used to find the designed variables for solving the VPS-HBM

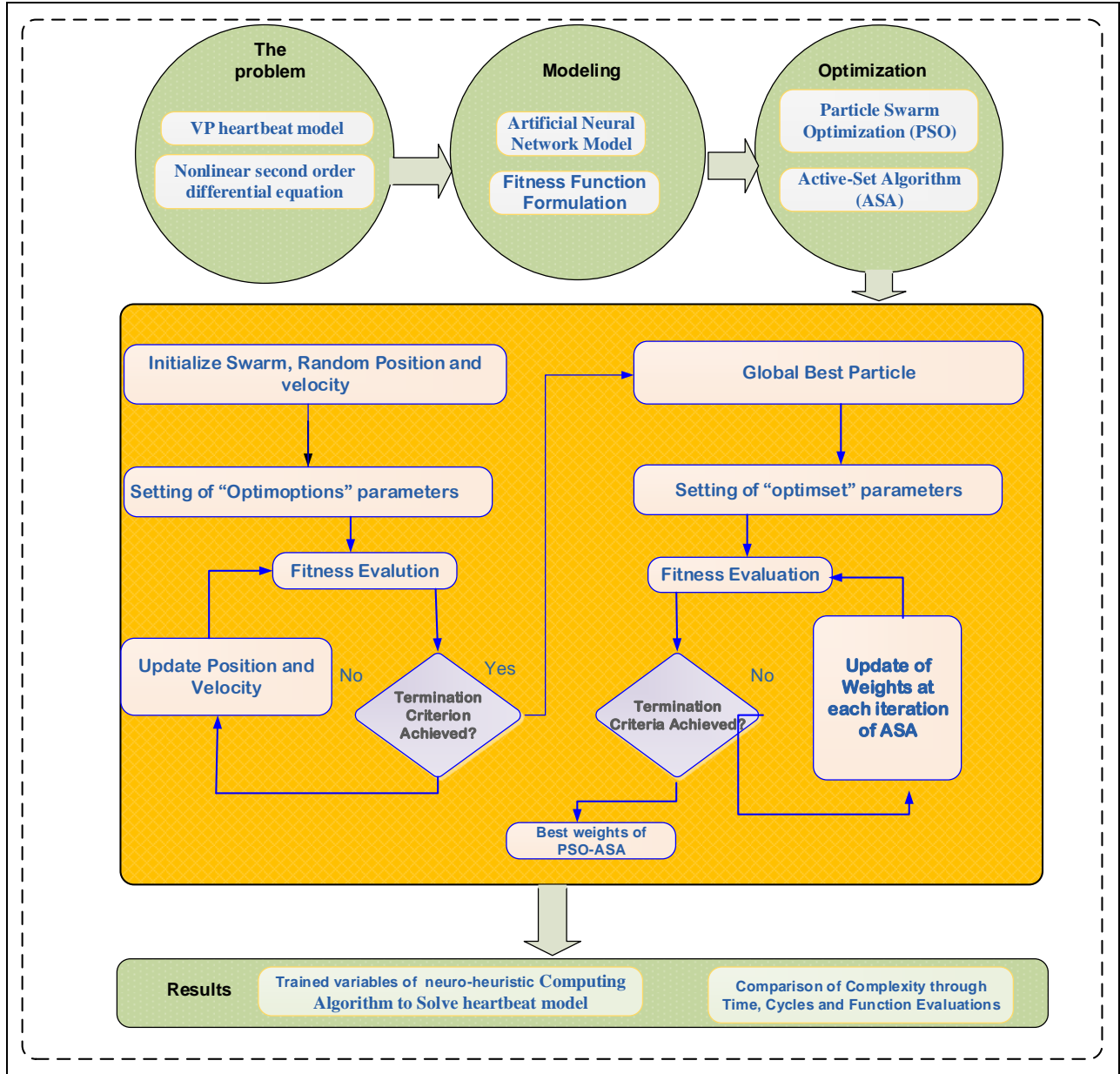


Figure 1: Graphical abstract of present scheme for VP system of heartbeat model

3. Performance indices

The performance analysis for VPS-HBM are constructed for mean absolute deviation (MAD), variance account for (VAF) and Theil's inequality coefficient (TIC). These performances are used to examine the designed methodologies of the model. The mathematical form of these operators MAD, VAF and TIC is given as

$$\text{MAD} = \sum_{j=1}^m |u_j - \hat{u}_j|, \quad (14)$$

$VAF = \left(1 - \frac{\text{var}(u - \hat{u})}{\text{var}(u)}\right) * 100,$	(15)
$EVAF = -(VAF - 100),$	(16)
$TIC = \frac{\sqrt{\frac{1}{m} \sum_{j=1}^m (u_j - \hat{u}_j)^2}}{\left(\sqrt{\frac{1}{m} \sum_{j=1}^m u_j^2} + \sqrt{\frac{1}{m} \sum_{j=1}^m \hat{u}_j^2} \right)}.$	(17)

Where j is the grid point, u and \hat{u} are used for the reference and approximate solutions.

Table 1: Pseudo code of optimization tool of PSO-ASA

<p>Particle Swarm procedure started</p> <p>Inputs:</p> <p style="padding-left: 20px;">The chromosome with same number of entries of the Networks as:</p> <p style="padding-left: 20px;">$\mathbf{W} = [\alpha, \xi, \beta]$</p> <p style="padding-left: 20px;">Population: The chromosomes set is symbolized as:</p> <p style="padding-left: 20px;">$\alpha = [\alpha_1, \alpha_2, \alpha_3, \dots, \alpha_m], \xi = [\xi_1, \xi_2, \xi_3, \dots, \xi_m]$ and $\beta = [\beta_1, \beta_2, \beta_3, \dots, \beta_m]$.</p> <p style="padding-left: 20px;">$\mathbf{P} = [W_1, W_2, \dots, W_m]^t$</p> <p>Output:</p> <p style="padding-left: 20px;">The Best Global-weights of PSO \mathbf{W}_{B-PSO}</p> <p>Initialization</p> <p style="padding-left: 20px;">Construct a \mathbf{W} (weight vector) of real bounded numbers to indicate a chromosome. Set of \mathbf{W} is used to form an initial \mathbf{P}. Generate randomly initial swarm of the particle by initializing the 'PSO' and 'gaoptimset' routines</p> <p>Fitness evaluation</p> <p style="padding-left: 20px;">Attained the fitness 'E' in 'P' for all 'W' by using equations (9) to (11)</p> <p>Termination</p> <p style="padding-left: 20px;">Terminate the process to achieve one of the following</p> <ul style="list-style-type: none"> • 'Fitness' $e \rightarrow 10^{-18}$, • 'TolFun' $\rightarrow 10^{-18}$, • 'Populationspan' $\rightarrow (-30, 30)$ • 'Initialweights' \rightarrow linearly decreasing • 'particlecize' $\rightarrow 30$ • 'SwarmSize' $\rightarrow 100$ • "HybridFcn" \rightarrow @fmincon • "Velocity span" $\rightarrow (-2, 2)$ • Other functions taken as default <p style="padding-left: 20px;">Go to step storage, when stopping criteria meets</p>	
--	--

Ranking
 Ranked each W of P for brilliance of E

Renewal
 Call the position and velocity using Eqs. (13-14)

'fitness evaluation' step

Storage
 Save W_{B-PSO} the best weight vector, fitness E , with its time, generation and function counts for the existent run of PSO

End Particle Swarm Optimization

PSO-ASA Procedure Start

Inputs
 Take W_{B-PSO} as a start point

Output
 Best weights of PSO-ASA is $W_{PSO-ASA}$

Initialize
 Use W_{B-PSO} as a start point
 Bounded constraints, total iterations, assignments and other decelerations

Terminate
 Algorithm stop when any of the following criteria meet
 'Fitness' $e \leq 10^{-14}$, 'total Iterations' = 900,
 'TolFun'' $\leq 10^{-20}$, 'TolX' $\leq 10^{-20}$, 'TolCon' $\leq 10^{-22}$,
 and 'MaxFunEvals' ≤ 250000
 While (Terminate required criteria fulfilled)

Fitness calculation
 Calculate E of the present W using Eqs (9-11)

Adjustments
 Invoking 'fmincon' for the PSO. Modify W for each generation of ASA. Compute E of updated W again using Eqs (5-7).

Accumulate
 Store the weight vector $W_{PSO-ASA}$ values, fitness E value, number of iterations, the time t , and count of function for the current runs of ASA.

PSO-ASA Procedure End

4. Numerical results and discussion

The numerical results for the present scheme are presented here for two problems of nonlinear VP heart model. Different values of asymmetric damping parameters, pulse shape variation factor a for each problem are taken. The comparison of the present solutions with reference numerical values of AM. To demonstrate the worth of the present design, numerical results are presented in the form of graphical illustrations as well as tabulated form.

Problem 1:

Consider the heartbeat dynamical VP model (1) have been taken by varying a , and different values of v_1 and v_2 . While e is fixed term that used to switch the period of atrial/ventricular contraction. The term d is used to exchange the harmonic forcing of standard VP model.

Scenario 1:

Heartbeat dynamics model is taken with three values of pulse shape modification factor a and is given as:

Cases	a	v_1	v_2	d	e	C_1	C_2
1	3	0.83	-0.83	3	6	-0.1	0.025
2	2	0.83	-0.83	3	6	-0.1	0.025
3	1	0.83	-0.83	3	6	-0.1	0.025

The heartbeat VP model for the above scenario is written as:

$\ddot{u} + a(u - 0.83)(u + 0.83)\dot{u} + \frac{u(u+3)(u+6)}{18} = 0,$	(18)
$u(0) = -0.1, \quad \dot{u}(0) = 0.025.$	

The fitness function for model (18) is written as:

$E = \frac{1}{N} \sum_{m=1}^N \left(\hat{u}_m + a(\hat{u}_m - 0.83)(\hat{u}_m + 0.83)\hat{u}_m + \frac{\hat{u}_m(\hat{u}_m + 3)(\hat{u}_m + 6)}{18} \right)^2$ $+ \frac{1}{2}(\hat{u}_m + 0.1)^2 + \frac{1}{2}(\hat{u}_m - 0.025)^2$	(19)
---	-------------

Scenario 2:

Changing the values of asymmetric damping factors (v_1, v_2)

Cases	a	v_1	v_2	d	e	C_1	C_2
1	2	0.93	-0.93	3	6	-0.1	0.025
2	2	0.43	-0.43	3	6	-0.1	0.025
3	2	0.63	-0.63	3	6	-0.1	0.025

The heartbeat VP model for the scenario (2) is written as:

$\ddot{u} + 2(u - v_1)(u - v_2)\dot{u} + \frac{u(u+3)(u+6)}{18} = 0,$	(20)
$u(0) = -0.1, \quad \dot{u}(0) = 0.025.$	

The fitness formulation of the model (20) is written as:

$E = \frac{1}{N} \sum_{m=1}^N \left(\hat{u}_m + 2(\hat{u}_m - v_1)(\hat{u}_m - v_2)\hat{u}_m + \frac{\hat{u}_m(\hat{u}_m + 3)(\hat{u}_m + 6)}{18} \right)^2$ $+ \frac{1}{2}(\hat{u}_m + 0.1)^2 + \frac{1}{2}(\hat{u}_m - 0.025)^2$	(21)
---	-------------

Optimization of above model is executed with the combination of PSO-ASA.

Scenario 3:

In this scenario, forcing factor $g(t) = B \sin(\psi t)$ based on the variation in pulse shape modification term a .

Cases	a	v_1	v_2	d	e	B	ψ	C_1	C_2
1	0.5	0.97	-1	3	6	2.5	1.9	-0.1	0.025
2	0.4	0.97	-1	3	6	2.5	1.9	-0.1	0.025
3	0.3	0.97	-1	3	6	2.5	1.9	-0.1	0.025

For the above scenario the model becomes as:

$\ddot{u} + a(u - 0.97)(u + 1)\dot{u} + \frac{u(u + 3)(u + 6)}{18} = 2.5 \sin(1.9t),$	(22)
$u(0) = -0.1, \quad \dot{u}(0) = 0.025.$	

The fitness function of the model (22) is written as:

$E = \frac{1}{N} \sum_{m=1}^N \left(\hat{u}_m + a(\hat{u}_m - 0.97)(\hat{u}_m + 1)\hat{u}_m + \frac{\hat{u}_m(\hat{u}_m + 3)(\hat{u}_m + 6)}{18} - 2.5 \sin(1.9t) \right)^2$ $+ \frac{1}{2}(\hat{u}_m + 0.1)^2 + \frac{1}{2}(\hat{u}_m - 0.025)^2$	(23)
---	-------------

Optimization of above model is executed with the combination of PSO-ASA. The proposed solutions are obtained by using the weights for scenarios (1-3)

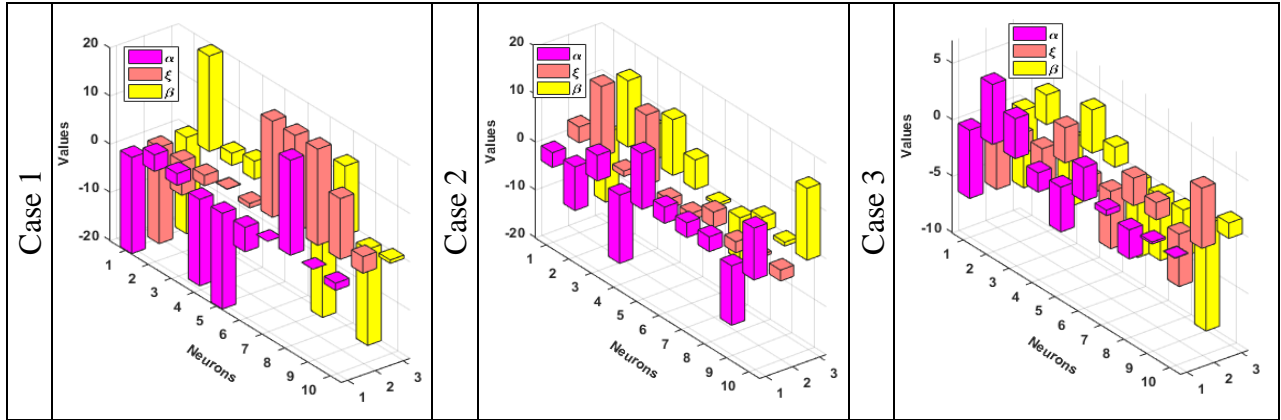


Figure 2: Set of weights for cases (1-3) of scenario 1

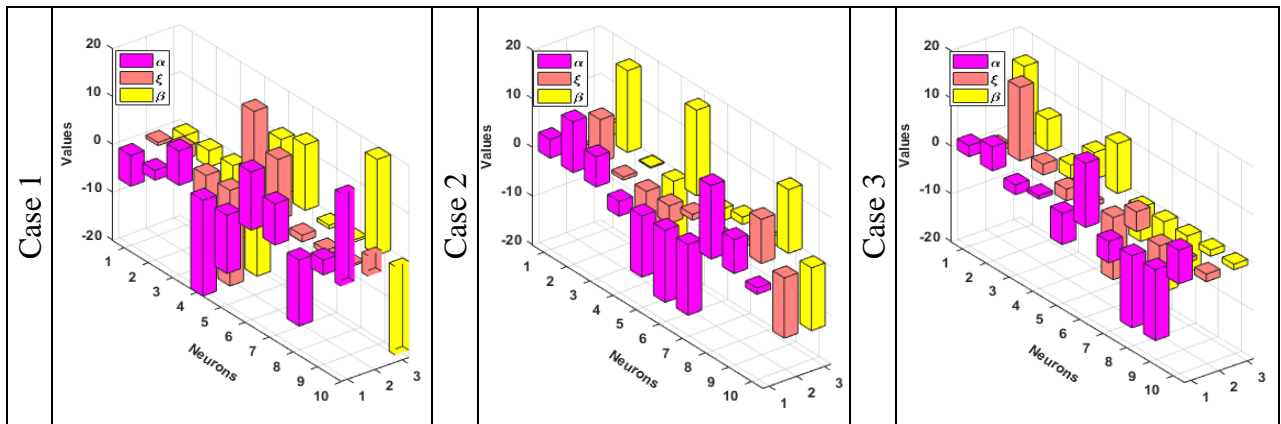


Figure 3: Set of weights for cases (1-3) of scenario 2

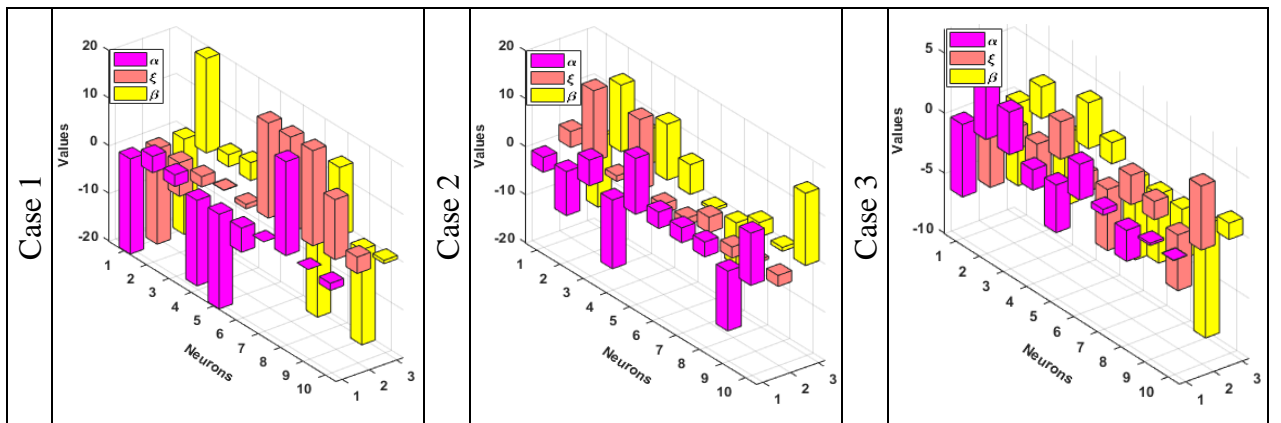


Figure 4: Set of weights for cases (1-3) of scenario 3

Comparison of result and absolute error (AE) of present solution from reference Adams results for scenarios (1-3) are shown in Figs. (5-7). It is seen that the numerical Adams results and presents results overlapped for all cases of scenarios (1-3). Moreover, the AE lies between the ranges of 10^{-05} to 10^{-07} , 10^{-04} to 10^{-05} for cases (1-3) of scenario 1 and 2. The accuracy is achieved 10^{-04} to 10^{-06} for cases (2-3), while the values for case 1 lie around 10^{-02} to 10^{-04} of scenario 3. To assess the convergence and accuracy of the present technique, hundred independent runs of PSO-ASA are performed. The numerical statistical values based on minimum (Min), median (Med) and semi interquartile range (SIR) operators for hundred runs are tabulated in Table 2 for cases (1-3) of scenario 1. It is observed that Min values lie in the ranges of 10^{-05} to 10^{-11} for case 1, while for

cases (2-3) the Min values lie around 10^{-06} to 10^{-11} . The Med values lie around 10^{-04} to 10^{-08} for all cases of scenario 1. However, the SIR values lie in good ranges for all cases of scenario 1 and found to be around 10^{-04} to 10^{-06} . Table 2 is based on the statistical values of scenario 2 for all the cases. As a result, satisfactory level of values have been achieved for all the cases of scenario 2 and 3. The Min values lie around 10^{-06} to 10^{-12} , 10^{-04} to 10^{-08} , 10^{-06} to 10^{-11} for cases (1-3). Whereas, the Med and SIR values for all cases lie in the ranges of 10^{-04} to 10^{-05} .

For the gages of performance indices of fitness (FIT), MAD, ENSE and TIC are plotted in Figs. The mathematical form of these operators is shown in equations (9), (14), (16) and (17). Near optimum values observed for all the performances that establish the value, worth and significance of the present scheme.

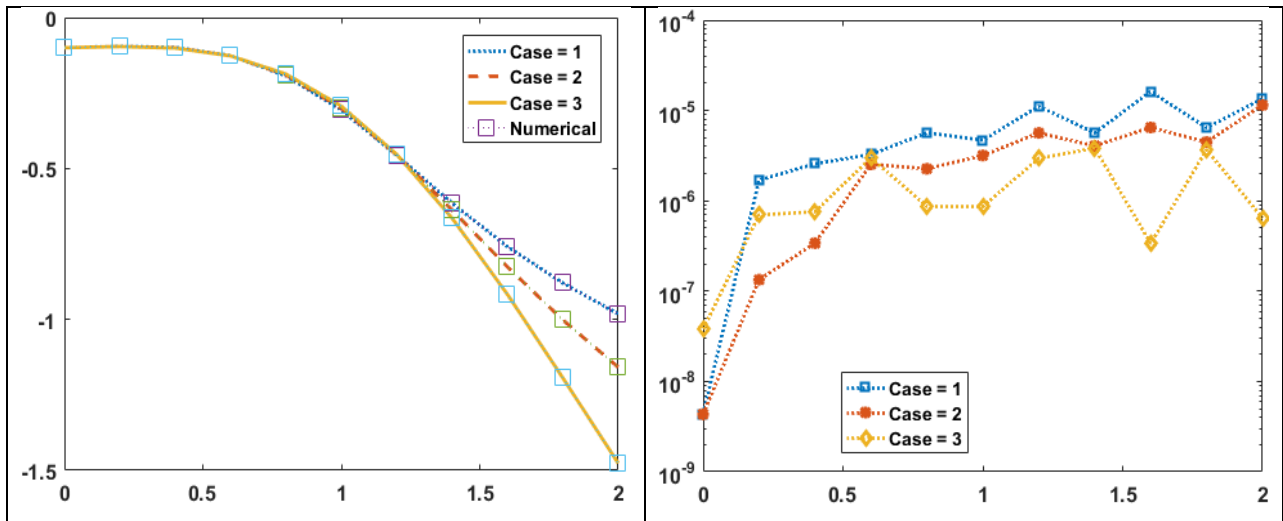


Figure 5: Comparison and AE of present solution from reference Adams results for cases (1-3) of scenario 1

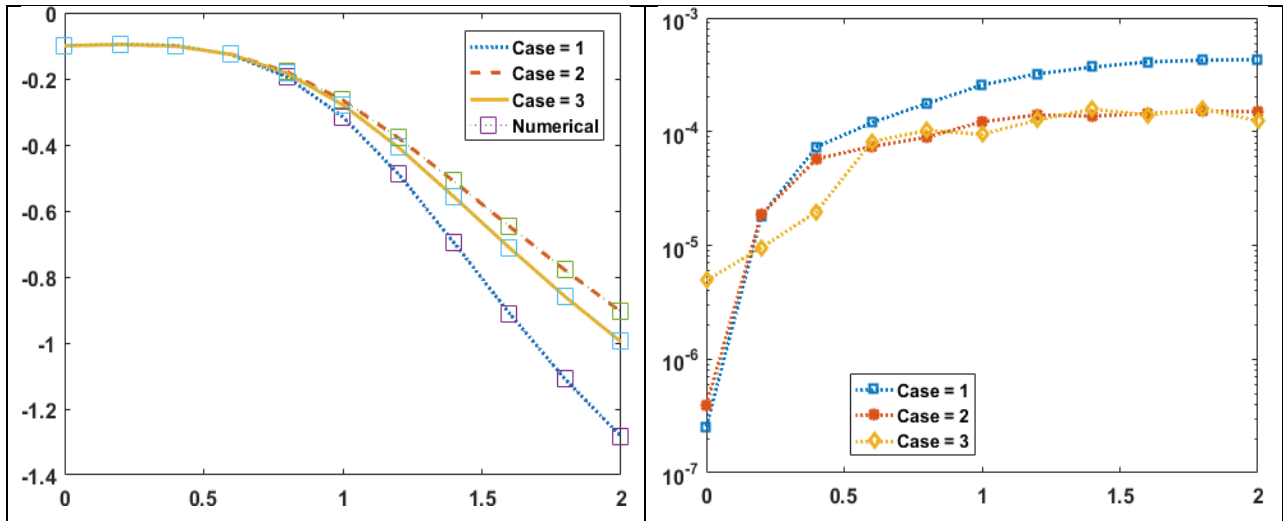


Figure 6: Comparison and AE of present solution from reference Adams results for cases (1-3) of scenario 2

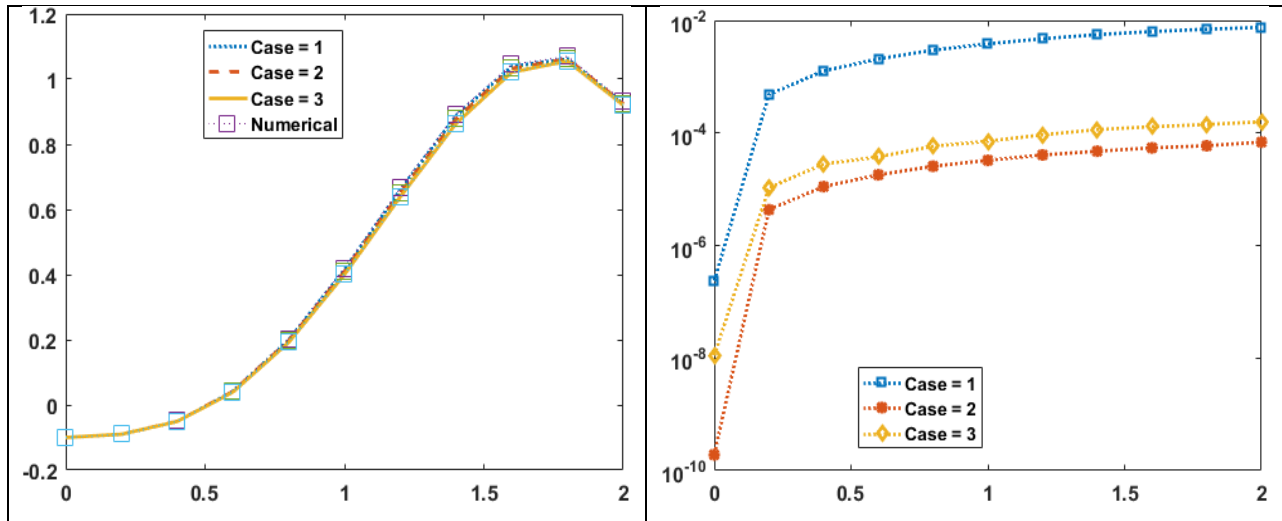


Figure 7: Comparison and AE of present solution from reference Adams results for cases (1-3) of scenario 3

Table 2: Comparison of statistical investigates of the present results for Scenario 1

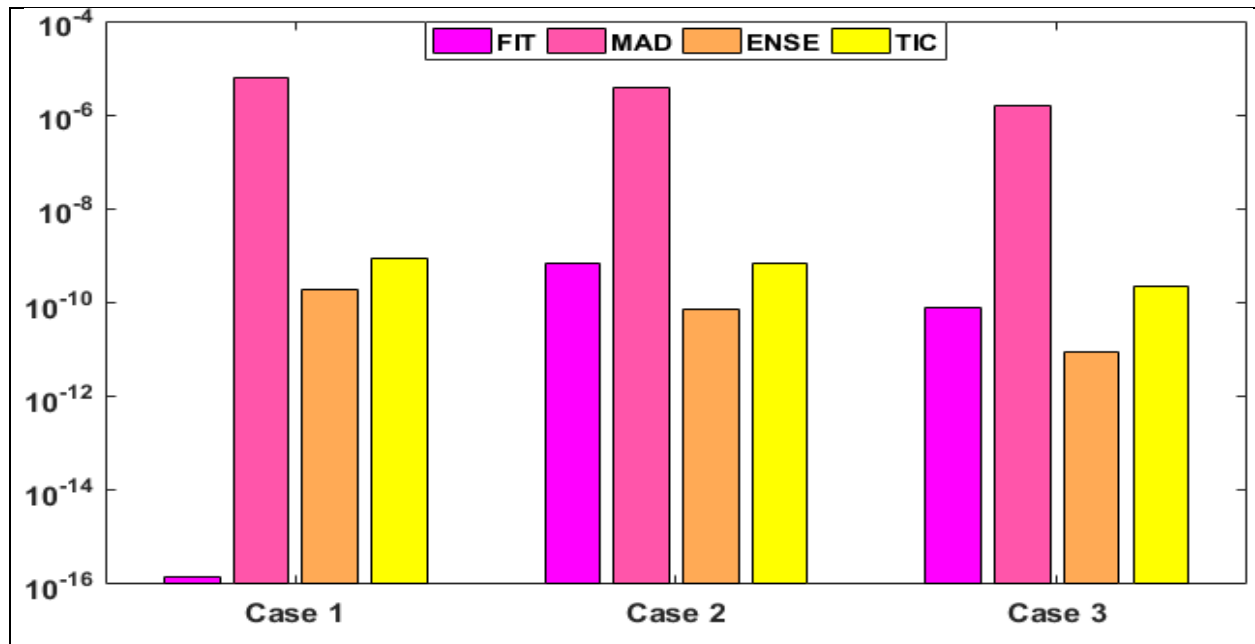
x	Case 1			Case 2			Case 3		
	Min	Median	SIR	Min	Median	SIR	Min	Median	SIR
0	9.03E-11	2.79E-08	1.06E-06	1.21E-11	2.83E-08	5.27E-07	6.33E-11	4.08E-08	1.30E-06
0.2	1.09E-06	3.06E-05	4.52E-05	1.34E-07	1.94E-05	2.64E-05	1.42E-07	1.22E-05	1.89E-05
0.4	2.57E-06	1.05E-04	1.48E-04	1.44E-07	7.47E-05	8.01E-05	7.57E-07	3.86E-05	4.43E-05
0.6	3.26E-06	1.90E-04	2.54E-04	2.42E-06	1.20E-04	1.35E-04	1.09E-06	5.88E-05	7.40E-05
0.8	5.67E-06	3.01E-04	3.94E-04	2.26E-06	1.81E-04	1.88E-04	8.65E-07	8.36E-05	1.01E-04
1	4.69E-06	4.12E-04	5.52E-04	2.84E-06	2.53E-04	2.26E-04	8.63E-07	1.10E-04	1.31E-04
1.2	1.07E-05	5.03E-04	6.72E-04	5.58E-06	2.99E-04	3.04E-04	2.25E-06	1.33E-04	1.66E-04
1.4	5.64E-06	5.64E-04	7.44E-04	4.05E-06	3.42E-04	3.45E-04	2.59E-06	1.52E-04	1.85E-04
1.6	1.23E-05	5.92E-04	7.87E-04	2.84E-06	3.69E-04	3.54E-04	3.37E-07	1.70E-04	2.05E-04
1.8	6.44E-06	6.01E-04	7.97E-04	4.46E-06	3.79E-04	3.78E-04	2.21E-06	1.80E-04	2.17E-04
2	1.08E-05	5.76E-04	8.04E-04	1.80E-06	3.64E-04	3.69E-04	6.43E-07	1.88E-04	2.41E-04

Table 3: Comparison of statistical investigates of the present results for Scenario 2

x	Case 1			Case 2			Case 3		
	Min	Median	SIR	Min	Median	SIR	Min	Median	SIR
0	1.68E-10	5.46E-08	1.76E-06	3.98E-11	7.91E-08	3.35E-06	1.52E-11	5.32E-08	1.06E-06
0.2	2.59E-07	2.25E-05	3.62E-05	4.76E-08	2.15E-05	3.12E-05	5.46E-07	2.51E-05	4.15E-05
0.4	6.74E-07	9.05E-05	1.10E-04	1.01E-06	6.47E-05	7.24E-05	1.51E-06	8.76E-05	1.13E-04
0.6	4.34E-06	1.50E-04	1.97E-04	9.71E-07	9.36E-05	9.19E-05	2.15E-06	1.15E-04	1.85E-04
0.8	8.82E-06	2.22E-04	3.15E-04	2.01E-06	1.33E-04	1.25E-04	2.97E-06	1.55E-04	2.63E-04
1	5.12E-06	3.19E-04	4.30E-04	2.99E-06	1.69E-04	1.45E-04	4.06E-06	2.18E-04	3.25E-04
1.2	1.03E-05	4.00E-04	5.47E-04	1.73E-06	1.82E-04	1.60E-04	3.44E-06	2.58E-04	3.82E-04
1.4	1.83E-05	4.58E-04	6.45E-04	1.19E-06	1.92E-04	1.78E-04	5.18E-06	2.51E-04	4.19E-04
1.6	1.28E-05	5.08E-04	6.93E-04	3.52E-06	2.07E-04	1.84E-04	5.20E-06	2.67E-04	4.32E-04
1.8	1.81E-05	5.27E-04	7.32E-04	3.06E-06	2.08E-04	1.80E-04	4.13E-06	2.93E-04	4.47E-04
2	1.13E-05	5.55E-04	7.25E-04	1.93E-06	1.97E-04	1.89E-04	5.13E-06	2.80E-04	4.38E-04

Table 4: Comparison of statistical investigates of the present results for Scenario 1

x	Case 1			Case 2			Case 3		
	Min	Median	SIR	Min	Median	SIR	Min	Median	SIR
0	7.41E-12	9.78E-09	4.44E-07	1.18E-11	1.04E-08	3.50E-07	7.34E-11	6.46E-09	2.55E-07
0.2	2.16E-07	2.43E-05	6.18E-05	1.30E-07	3.60E-05	7.28E-05	1.17E-07	3.20E-05	6.73E-05
0.4	5.98E-07	6.42E-05	1.48E-04	4.51E-07	9.00E-05	1.89E-04	6.30E-07	8.20E-05	1.73E-04
0.6	1.09E-06	1.03E-04	2.32E-04	8.09E-07	1.40E-04	3.10E-04	6.63E-07	1.31E-04	2.81E-04
0.8	1.39E-06	1.48E-04	3.28E-04	1.12E-06	2.06E-04	4.38E-04	1.19E-06	1.85E-04	3.94E-04
1	2.21E-06	1.91E-04	4.29E-04	1.81E-06	2.63E-04	5.68E-04	1.43E-06	2.36E-04	5.06E-04
1.2	2.43E-06	2.36E-04	5.22E-04	1.90E-06	3.14E-04	6.98E-04	1.61E-06	2.90E-04	6.21E-04
1.4	3.18E-06	2.79E-04	6.11E-04	2.52E-06	3.78E-04	8.22E-04	2.02E-06	3.41E-04	7.32E-04
1.6	2.86E-06	3.15E-04	6.98E-04	2.69E-06	4.23E-04	9.37E-04	2.24E-06	3.89E-04	8.34E-04
1.8	4.35E-06	3.48E-04	7.64E-04	3.52E-06	4.74E-04	1.04E-03	2.46E-06	4.33E-04	9.29E-04
2	3.53E-06	3.76E-04	8.24E-04	7.05E-07	5.01E-04	1.11E-03	2.64E-06	4.75E-04	1.01E-03

**Figure 8:** The magnitude of performance indices for Case (1-3) of scenario 1

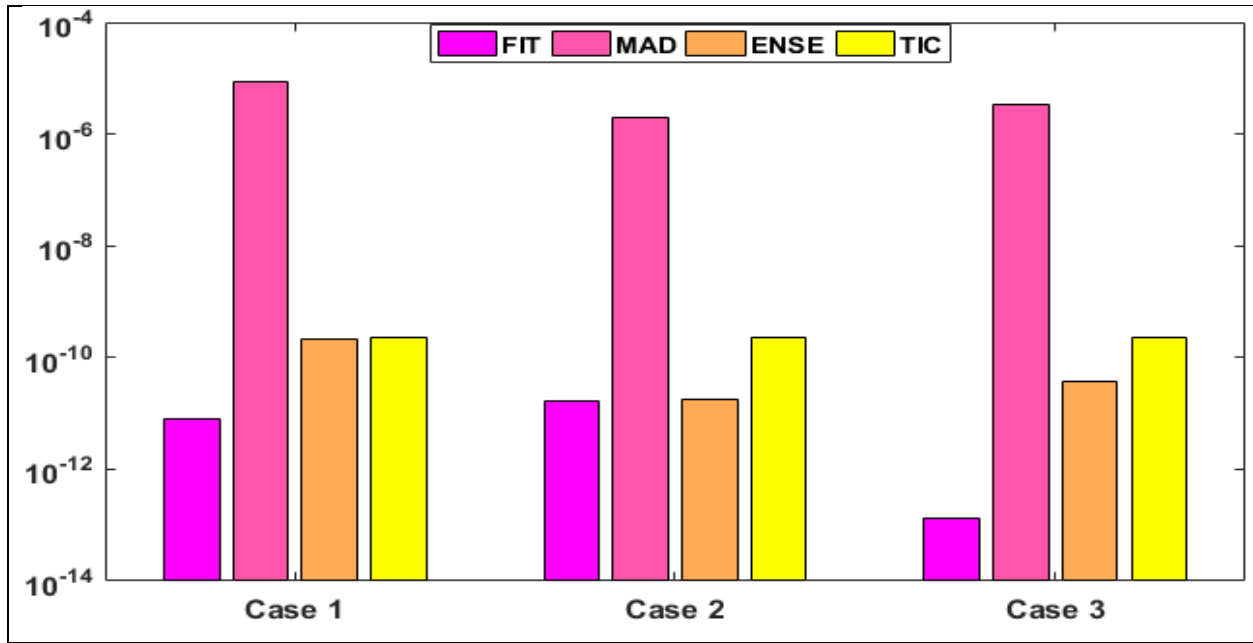


Figure 9: The magnitude of performance indices for Case (1-3) of scenario 2

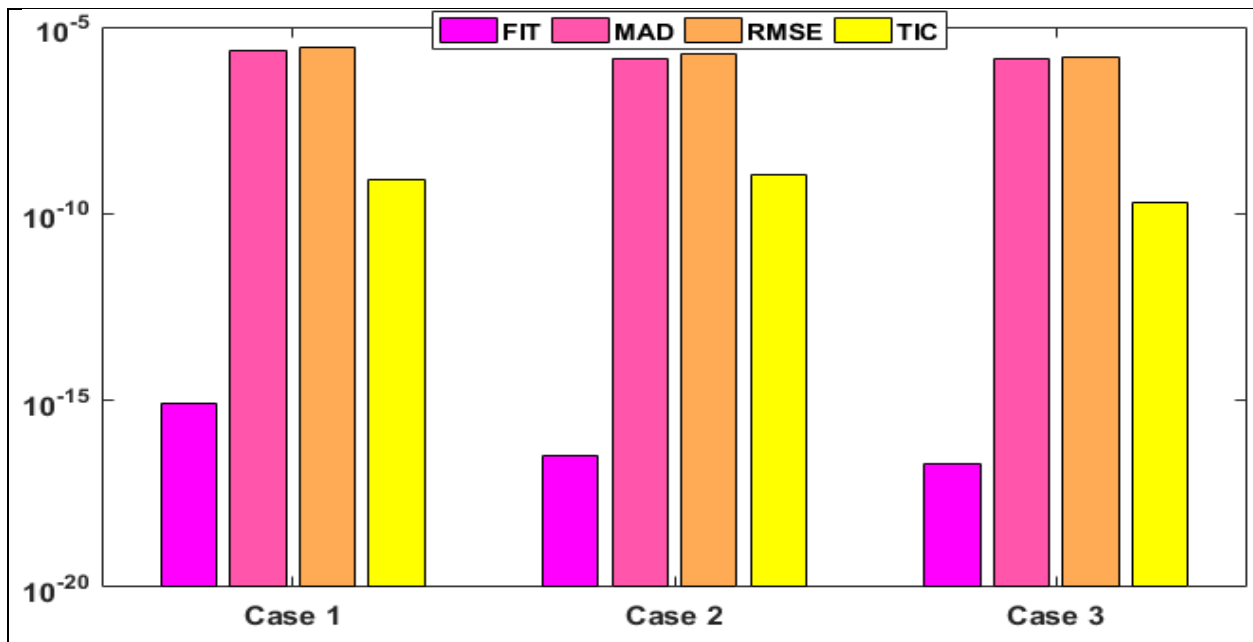


Figure 10: The magnitude of performance indices for Case (1-3) of scenario 3

Conclusion

Following conclusions have been drawn based on numerical experimentation

- Artificial neural network successfully applied for solving nonlinear Van der Pol system of heartbeat model numerically.
- Present numerical solutions for the model are much closer with the Adams numerical results.

- The efficiency of the present algorithm is analysed using the statistical gages based on median and semi interquartile range, and results of absolute error almost all the cases of model are found to very close to zero which shows the reliable accuracy of the present scheme.
- Convergence and accuracy of the present scheme is authenticated through steadily achieved the optimal values of performance operators based on MAD, ENSE and TIC in each case of the dynamical heartbeat model.

References

- [1] Hall, Kevin, et al. "Dynamic control of cardiac alternans." *Physical Review Letters* 78.23 (1997): 4518.
- [2] Grudziński, Krzysztof, and Jan J. Żebrowski. "Modeling cardiac pacemakers with relaxation oscillators." *Physica A: statistical Mechanics and its Applications* 336.1-2 (2004): 153-162.
- [3] dos Santos, Angela M., Sergio R. Lopes, and RL Ricardo L. Viana. "Rhythm synchronization and chaotic modulation of coupled Van der Pol oscillators in a model for the heartbeat." *Physica A: Statistical Mechanics and its Applications* 338.3-4 (2004): 335-355.
- [4] Ferreira, Bianca Borem, Aline Souza de Paula, and Marcelo Amorim Savi. "Chaos control applied to heart rhythm dynamics." *Chaos, Solitons & Fractals* 44.8 (2011): 587-599.
- [5] Shukla, Anant Kant, T. R. Ramamohan, and S. Srinivas. "A new analytical approach for limit cycles and quasi-periodic solutions of nonlinear oscillators: the example of the forced Van der Pol Duffing oscillator." *Physica Scripta* 89.7 (2014): 075202.
- [6] Chen, Y. M., and J. K. Liu. "A study of homotopy analysis method for limit cycle of van der Pol equation." *Communications in Nonlinear Science and Numerical Simulation* 14.5 (2009): 1816-1821.
- [7] Kimiaefar, A., et al. "Analysis of modified Van der Pol's oscillator using He's parameter-expanding methods." *Current Applied Physics* 10.1 (2010): 279-283.
- [8] Motsa, Sandile S., and Precious Sibanda. "A note on the solutions of the Van der Pol and Duffing equations using a linearisation method." *Mathematical Problems in Engineering* 2012 (2012).
- [9] Khan, Yasir, et al. "A new approach to Van der Pol's oscillator problem." *Zeitschrift für Naturforschung A* 66.10-11 (2011): 620-624.
- [10] Kumar, Manoj, and Neha Yadav. "Numerical solution of Bratu's problem using multilayer perceptron neural network method." *National Academy Science Letters* 38.5 (2015): 425-428.
- [11] Yadav, Neha, et al. "An efficient algorithm based on artificial neural networks and particle swarm optimization for solution of nonlinear Troesch's problem." *Neural Computing and Applications* 28.1 (2017): 171-178.
- [12] Patan, Krzysztof. "Local stability conditions for discrete-time cascade locally recurrent neural networks." *International Journal of Applied Mathematics and Computer Science* 20.1 (2010): 23-34.

- [13] Ewert, Paweł. "Application of neural networks to detect eccentricity of induction motors." *Power Electronics and Drives* 2.2 (2017): 151-165.
- [14] Pan, Lisheng. "Exploration and Mining Learning Robot of Autonomous Marine Resources Based on Adaptive Neural Network Controller." *Polish Maritime Research* 25.s3 (2018): 78-83.
- [15] Momani, Shaher, Zaer S. Abo-Hammour, and Othman MK Alsmadi. "Solution of inverse kinematics problem using genetic algorithms." *Applied Mathematics & Information Sciences* 10.1 (2016): 225.
- [16] Schaff, James C., et al. "Numerical approach to spatial deterministic-stochastic models arising in cell biology." *PLoS computational biology* 12.12 (2016): e1005236.
- [17] Raja, Muhammad Asif Zahoor, et al. "Design of artificial neural network models optimized with sequential quadratic programming to study the dynamics of nonlinear Troesch's problem arising in plasma physics." *Neural Computing and Applications* 29.6 (2018): 83-109.
- [18] Umar, Muhammad, Zulqurnain Sabir, and Muhammad Asif Zahoor Raja. "Intelligent computing for numerical treatment of nonlinear prey–predator models." *Applied Soft Computing* 80 (2019): 506-524.
- [19] Pelletier, Francis, Christian Masson, and Antoine Tahan. "Wind turbine power curve modelling using artificial neural network." *Renewable Energy* 89 (2016): 207-214.
- [20] Soize, Christian. "Stochastic models of uncertainties in computational structural dynamics and structural acoustics." *Nondeterministic Mechanics*. Springer, Vienna, 2012. 61-113.
- [21] Raja, Muhammad Asif Zahoor, Junaid Ali Khan, and Tahira Haroon. "Stochastic numerical treatment for thin film flow of third grade fluid using unsupervised neural networks." *Journal of the Taiwan Institute of Chemical Engineers* 48 (2015): 26-39.
- [22] Sabir, Zulqurnain, et al. "Neuro-heuristics for nonlinear singular Thomas-Fermi systems." *Applied Soft Computing* 65 (2018): 152-169.
- [23] Effati, Sohrab, and Morteza Pakdaman. "Artificial neural network approach for solving fuzzy differential equations." *Information Sciences* 180.8 (2010): 1434-1457.
- [24] Raja, Muhammad Asif Zahoor, et al. "A new stochastic computing paradigm for the dynamics of nonlinear singular heat conduction model of the human head." *The European Physical Journal Plus* 133.9 (2018): 364.
- [25] Raja, Muhammad Asif Zahoor, et al. "Numerical solution of doubly singular nonlinear systems using neural networks-based integrated intelligent computing." *Neural Computing and Applications* 31.3 (2019): 793-812.
- [26] Zhang, Zheng, et al. "Stochastic testing method for transistor-level uncertainty quantification based on generalized polynomial chaos." *IEEE Transactions on Computer-Aided Design of Integrated Circuits and Systems* 32.10 (2013): 1533-1545.
- [27] Raja, Muhammad Asif Zahoor, et al. "Stochastic numerical solver for nanofluidic problems containing multi-walled carbon nanotubes." *Applied Soft Computing* 38 (2016): 561-586.

- [28] Sabir, Z., and M. Raja. "Numeric treatment of nonlinear second order multi-point boundary value problems using ANN, GAs and sequential quadratic programming technique." *International Journal of Industrial Engineering Computations* 5.3 (2014): 431-442.
- [29] He, Wei, Yuhao Chen, and Zhao Yin. "Adaptive neural network control of an uncertain robot with full-state constraints." *IEEE transactions on cybernetics* 46.3 (2016): 620-629.
- [30] Manik, Shubham, Lalit Mohan Saini, and Nikhil Vadera. "Counting and classification of white blood cell using artificial neural network (ANN)." *2016 IEEE 1st International Conference on Power Electronics, Intelligent Control and Energy Systems (ICPEICES)*. IEEE, 2016.
- [31] Van Der Pol, Balth, and Jan Van Der Mark. "LXXII. The heartbeat considered as a relaxation oscillation, and an electrical model of the heart." *The London, Edinburgh, and Dublin Philosophical Magazine and Journal of Science* 6.38 (1928): 763-775.
- [32] Ge, Zheng-Ming, and Mao-Yuan Hsu. "Chaos in a generalized van der Pol system and in its fractional order system." *Chaos, Solitons & Fractals* 33.5 (2007): 1711-1745.
- [33] Effati, Sohrab, and Mohammad Hadi Noori Skandari. "Optimal control approach for solving linear Volterra integral equations." *International Journal of Intelligent Systems and Applications* 4.4 (2012): 40.
- [34] Shi, Yuhui, and Russell C. Eberhart. "Empirical study of particle swarm optimization." *Proceedings of the 1999 Congress on Evolutionary Computation-CEC99 (Cat. No. 99TH8406)*. Vol. 3. IEEE, 1999.
- [35] Engelbrecht, Andries P. *Computational intelligence: an introduction*. John Wiley & Sons, 2007.
- [36] Shen, Meie, et al. "Bi-velocity discrete particle swarm optimization and its application to multicast routing problem in communication networks." *IEEE Transactions on Industrial Electronics* 61.12 (2014): 7141-7151.
- [37] Khare, Anula, and Saroj Rangnekar. "A review of particle swarm optimization and its applications in solar photovoltaic system." *Applied Soft Computing* 13.5 (2013): 2997-3006.
- [38] Esmin, Ahmed AA, Rodrigo A. Coelho, and Stan Matwin. "A review on particle swarm optimization algorithm and its variants to clustering high-dimensional data." *Artificial Intelligence Review* 44.1 (2015): 23-45.
- [39] Akay, Bahriye. "A study on particle swarm optimization and artificial bee colony algorithms for multilevel thresholding." *Applied Soft Computing* 13.6 (2013): 3066-3091.
- [40] Soares, João, et al. "Application-Specific Modified Particle Swarm Optimization for energy resource scheduling considering vehicle-to-grid." *Applied Soft Computing* 13.11 (2013): 4264-4280.
- [41] Alba, Enrique, et al. "Gene selection in cancer classification using PSO/SVM and GA/SVM hybrid algorithms." *2007 IEEE Congress on Evolutionary Computation*. IEEE, 2007.
- [42] Lee, Ki-Baek, and Jong-Hwan Kim. "Multiobjective particle swarm optimization with preference-based sort and its application to path following footstep optimization for humanoid robots." *IEEE Transactions on Evolutionary Computation* 17.6 (2013): 755-766.

- [43] Doctor, Sheetal, Ganesh K. Venayagamoorthy, and Venu G. Gudise. "Optimal PSO for collective robotic search applications." Proceedings of the 2004 Congress on Evolutionary Computation (IEEE Cat. No. 04TH8753), Vol. 2. IEEE, 2004.
- [44] Koehler, Sarah, Claus Danielson, and Francesco Borrelli. "A primal-dual active-set method for distributed model predictive control." Optimal Control Applications and Methods 38.3 (2017): 399-419.
- [45] Quirynen, Rien, Andrew Knyazev, and Stefano Di Cairano. "Block structured preconditioning within an active-set method for real-time optimal control." 2018 European Control Conference (ECC). IEEE, 2018.
- [46] Li, Yong, Gonglin Yuan, and Zhou Sheng. "An active-set algorithm for solving large-scale nonsmooth optimization models with box constraints." PloS one 13.1 (2018): e0189290.
- [47] Friedrich, Johannes, and Liam Paninski. "Fast active set methods for online spike inference from calcium imaging." Advances In Neural Information Processing Systems. 2016.
- [48] Myre, Joe M., et al. "TNT-NN: a fast active set method for solving large non-negative least squares problems." Procedia Computer Science 108 (2017): 755-764.